*Journal of Applied Electrochemistry* **32**: 527–535, 2002.



# Corrosion inhibition of steel in chloride-containing alkaline solutions

C. MONTICELLI*, A. FRIGNANI and G. TRABANELLI
*Corrosion Study Centre "A. Daccò", Chemistry Department, University of Ferrara, via L. Borsari, 46-I-44100 Ferrara, Italy*
*(*author for correspondence)*

Received 3 August 2001; accepted in revised form 29 January 2002

*Key words:* chlorides, corrosion inhibition, EIS, FTIR, steel

**Abstract**

Some organic inhibitors of steel corrosion in saturated calcium hydroxide solutions containing 0.1 M chlorides were investigated to elucidate their interactions with the steel surface. The compounds studied were dicyclohexylammonium nitrite (DCHAMN), dicyclohexylamine (DCHA), sodium β-glycerophosphate (GPH) and 5-hexyl-benzotriazole (C6BTA). Sodium nitrite (SN) was also studied as a reference. The techniques applied were electrochemical impedance spectroscopy (EIS), polarization curves, cyclic voltammetry (CV) and Fourier transform infrared (FTIR) spectroscopy.

FTIR spectra showed that DCHAMN, DCHA, GPH and C6BTA interact with the steel surface by chemisorption and some information about the mechanism also emerged. From DCHAMN solution, DCHA chemisorption is induced by slow salt hydrolysis. CV tests show that, among chemisorbed substances, only GPH avoids chloride penetration on cycling, most likely due to a quick chemisorption, while DCHAMN can only enlarge the passive potential range. Addition of SN also prevents chloride attack on cycling.

Twenty days of immersion in inhibited solutions revealed that, besides SN, GPH and DCHAMN also form an impervious surface film on steel, which blocks any localized corrosion attack, whereas in the case of DCHA and C6BTA solutions, pitting corrosion is slowed down, but not avoided. DCHAMN exhibits the highest inhibiting efficiency at long immersion times, as a result of a synergetic inhibitive action which develops between nitrite and chemisorbed DCHA.

## 1. Introduction

Calcium nitrite is the most common commercial inhibitor used to prevent steel rebar corrosion in concrete. Owing to its anodic inhibitor nature and its toxicity, alternative substance types, either organic or inorganic, are currently under test to replace it [1].

A study was carried out in this laboratory [2] to assess the inhibitive properties of various substances towards steel corrosion in chloride-polluted steel-reinforced mortars. The substances were firstly screened to evaluate their inhibiting efficiencies during 30-day immersions in saturated calcium hydroxide solution, containing 0.1 M chloride ions. Besides 0.05 M sodium nitrite (SN), only 0.05 M sodium β-glycerophosphate (GPH), 0.005 M 5-hexyl-benzotriazole (C6BTA), saturated dicyclohexylammonium nitrite (DCHAMN) and dicyclohexylamine (DCHA) were able to inhibit the steel corrosion process and slow pitting corrosion more or less efficiently.

The present study was undertaken to investigate the inhibition mechanism of SN, GPH, C6BTA, DCHAMN and DCHA in chloride containing alkaline solutions. Their properties were investigated by both electrochemical tests (polarization curve recording, EIS, CV) and FTIR spectroscopy.

## 2. Experimental details

Specimens for electrochemical tests were cut from AISI 1033 bars (chemical composition: 0.3% C; 0.03% S; <0.01% P; 0.04% Si; 0.96% Mn; 0.2% Ni; 0.02% Cu; 0.07% Al; balance Fe), currently used as concrete reinforcement. Steel sheets of similar compositions were used for FTIR spectroscopy. The specimens used for electrochemical tests were discs embedded in epoxy (exposed surface area 0.8 $cm^2$).

The specimen surfaces were always prepared by surface grinding with emery paper from no. 120 to no. 600. The sheets were also polished on one side, down to 1 $\mu$m roughness. Finally, the specimens were washed with double distilled water and degreased with acetone.

The test solution was prepared by dissolving 0.05 M $CaCl_2$ in saturated calcium hydroxide solution. DCHAMN and DCHA were used under saturated conditions (about 0.05 M for the former additive) and

C6BTA was studied at a concentration of 0.005 M (close to the substance saturated conditions). GPH or SN solution concentrations were always 0.05 M.

Electrochemical impedance spectroscopy (EIS) tests were carried out in chloride-polluted solutions using a Solartron 1260/1287 FRA/Electrochemical Interface and a IBM compatible PC for data logging and analysis. The measurements were recorded at the corrosion potential, by applying a ±10 mV r.m.s. sinusoidal perturbation at frequencies ranging from $10^4$ Hz $10^{-2}$ Hz. Spectra were collected after 1, 7 and 20 days of immersion. The experimental data were processed by ZPlot for Windows® software [3]. Besides resistance and capacitance elements, constant phase elements (CPE) and generalized finite Warburg elements ($W_1$) were also included in the equivalent circuits to fit the experimental spectra.

The constant phase element (CPE) is a simple distributed element with an impedance expression $Z_{CPE} = 1/[C(i\omega)^P]$. It produces an impedance with a constant phase angle $P(\pi/2)$, in the complex plane ($0 \le P \le 1$). In the special case of $P = 1$, the CPE is an effective capacitance $C$.

The impedance expression for the generalized finite Warburg element ($W_1$) is

$$Z_{W1} = R\,\mathrm{tgh}[(iT\omega)^P]/(iT\omega)^P$$

where $\omega = 2\pi f$ (rad $s^{-1}$), $i = \sqrt{(-1)}$ and the parameters $R$ ($\Omega cm^2$), $T$ ($s^{-1}$) and $P$ ($0 \le P \le 1$) are coefficients of the generalized finite Warburg element. $T$ corresponds to $L^2/D$ (where $L$ is the effective diffusion thickness, and $D$ is the effective diffusion coefficient of the species). Polarization curves were recorded after 45 min and 20 days of immersion in uninhibited and inhibited solutions, starting from the corrosion potential (scan rate 0.1 mV $s^{-1}$). Cyclic voltammetry (CV) was run between −1.4 and +0.55 V in aerated conditions (scan rate 10 mV $s^{-1}$). All the potentials quoted in the text refer to the saturated calomel electrode (SCE).

Fourier transform infrared (FTIR) spectroscopy was applied after a three-day immersion of the steel sheets in saturated calcium hydroxide solution, both in the absence and presence of the different inhibitors. Before the tests, the steel sheets were thoroughly rinsed with bidistilled water and dried. Diffuse reflectance spectra were recorded on KBr powder, previously rubbed on the specimen surfaces to partially remove the surface film. A mercury cadmium telluride (MCT) detector was usually adopted, given its high sensitivity.

## 3. Results

### 3.1. *EIS spectra*

In the blank solution, under free corrosion conditions, a localized corrosion attack developed within a few hours following immersion. The impedance spectra recorded after 1, 7 or 20 day immersions are shown in Figure 1.

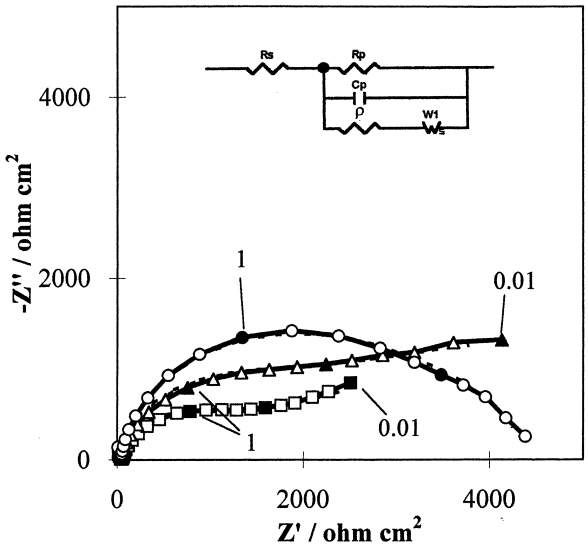


*Fig. 1.* EIS spectra obtained in blank solution after 1 (○), 7 (△) and 20 (□) days of immersion. Solid symbols refer to integer frequency decades. Simulations (dotted lines) by equivalent circuit in Figure 1 are also included.

All of them show the presence of two time constants, more or less clearly resolved.

Even in the presence of DCHA or C6BTA, two time constants were noticed, better resolved at short immersion times. As an example Figure 2 shows the spectra obtained in DCHA solution. Both additives were able to delay the development of pitting corrosion at long immersion times, but could not prevent it completely.

In contrast, in the presence of SN, DCHAMN or GPH localized corrosion was prevented throughout the immersion period. The spectra exhibited only one time constant at all immersion times, as shown in Figure 3, for the case of DCHAMN.

The equivalent circuit fitting the spectra collected in Figure 1 (where the circuit scheme is included) consisted

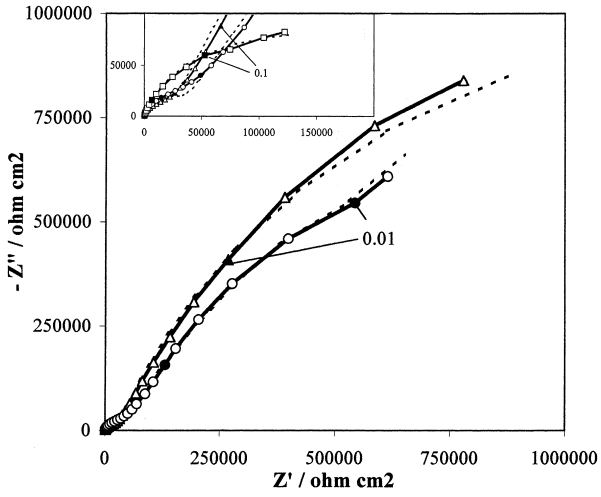


*Fig. 2.* EIS spectra obtained in DCHA solution after 1 (○), 7 (△) and 20 (□) days of immersion. Solid symbols refer to integer frequency decades. Simulations (dotted lines) by equivalent circuit in Figure 1 are also included.

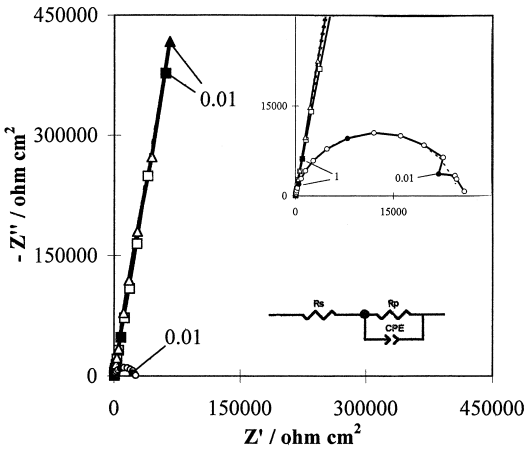


*Fig. 3.* EIS spectra obtained in DCHAMN solution, after 1 (○), 7 (△) and 20 (□) days of immersion. Solid symbols refer to integer frequency decades. Simulations (dotted lines) by equivalent circuit in Figure 3 are also included.

in a resistance $R_s$ (solution resistance), in series with three parallel arms, containing a resistance ($R_p$), a capacitance ($C_p$) and a resistance ($\rho$), respectively, in series to a generalized finite Warburg element ($W_1$). An analogous circuit was used for carbon steel in neutral chloride solutions, where a 0.5 fixed $P$ value was adopted [4, 5]. The same circuit can be used to fit the spectra collected in DCHA and C6BTA solutions.

The equivalent circuit fitting the impedance data in the presence of the most efficient inhibitors (DCHAMN, GPH and SN) is included in Figure 3. The third parallel arm was eliminated and $C_p$ substituted by a constant phase element (CPE). The parameters fitting the experimental data are reported in Tables 1 and 2 and the curves fitting the experimental data of Figures 1–3 are included in the Figures as dotted lines.

### 3.2. *Polarization curves*

Figure 4 shows the polarization curves obtained in the blank solution after immersions of 45 min (dotted lines) and 20 days. Pitting corrosion was induced during the anodic polarization, at short immersion times, while it was already present before the recording of the anodic curve obtained after long immersion times. This would explain the active $E_{cor}$ value and the relatively high passive current densities of the latter curve, although a kind of pseudopassivity persisted. The corresponding cathodic current densities of oxygen reduction were also slightly stimulated.

In Figure 5 the corrosion behaviour of steel in the presence of DCHAMN and DCHA is compared, at both immersion times. After a 45 min immersion, DCHAMN exhibited an anodic curve which was not very different from that of the blank, while after a 20 day immersion, DCHAMN contributed to the for-

*Table 1.* Parameters of the equivalent circuit (reported in Figure 1), fitting the experimental impedance spectra

| Environment | Immersion time/days | $E_{cor}$ /$V_{SCE}$ | $R_s$ /Ω cm$^2$ | $R_p$ /Ω cm$^2$ | $C_p$ μF cm$^{-2}$ | $\rho$ /Ω cm$^2$ | $R_{W1}$ /Ω cm$^2$ | $T_{W1}$ /s | $P_{W1}$ | Presence of localized attack |
|---|---|---|---|---|---|---|---|---|---|---|
| Blank = B | 1 | −0.496 | 42 | $4.9 \times 10^3$ | 40 | 10 | $3.7 \times 10^4$ | 24 | 0.42 | Y |
| | 7 | −0.550 | 42 | $1.8 \times 10^4$ | 100 | 270 | $1.4 \times 10^4$ | 1000 | 0.26 | Y |
| | 20 | −0.580 | 56 | $2.0 \times 10^4$ | 80 | 300 | $1.0 \times 10^4$ | 5000 | 0.24 | Y |
| B + C6BTA | 1 | −0.355 | 27 | $4.3 \times 10^5$ | 0.10 | 5000 | $5.0 \times 10^6$ | 430 | 0.81 | N |
| | 7 | – | – | – | – | – | – | – | – | – |
| | 20 | −0.415 | 40 | $2.8 \times 10^4$ | 1.0 | 10 | $6.3 \times 10^5$ | 270 | 0.85 | Y |
| B + DCHA | 1 | 0.075 | 40 | $3.0 \times 10^6$ | 0.24 | $3.5 \times 10^4$ | $4.1 \times 10^6$ | 150 | 0.68 | N |
| | 7 | 0.008 | 50 | $6.0 \times 10^6$ | 0.55 | $2.5 \times 10^4$ | $5.0 \times 10^6$ | 480 | 0.68 | N |
| | 20 | −0.367 | 60 | $2.0 \times 10^5$ | 1.9 | 42 | $1.0 \times 10^6$ | 26 | 0.75 | Y |

*Table 2.* Parameters of the equivalent circuits (reported in Figure 3) fitting the experimental impedance spectra
For steel in saturated calcium hydroxide solution, 20 days of immersion, the following parameters are found [14]: $R_s = 93$ Ω cm$^2$; $R_p = 1.2 \times 10^6$ Ω cm$^2$; $C_p = 25$ μF cm$^{-2}$; $P = 1$

| Environment | Immersion time /days | $E_{cor}$ /$V_{SCE}$ | $R_s$ /Ω cm$^2$ | $R_p$ /Ω cm$^2$ | $C_p$ /μF cm$^{-2}$ | $P$ | Presence of localized attack |
|---|---|---|---|---|---|---|---|
| B + DCHAMN | 1 | −0.250 | 39 | $2.5 \times 10^4$ | 96 | 0.89 | N |
| | 7 | −0.158 | 32 | $2.5 \times 10^7$ | 29 | 0.91 | N |
| | 20 | −0.008 | 32 | $6.1 \times 10^7$ | 31 | 0.90 | N |
| B + GPH | 1 | −0.317 | 19 | $2.3 \times 10^6$ | 27 | 0.94 | N |
| | 7 | −0.330 | 21 | $4.5 \times 10^6$ | 25 | 0.93 | N |
| | 20 | −0.186 | 12 | $8.7 \times 10^6$ | 41 | 0.93 | N |
| B + SN | 1 | −0.261 | 20 | $6.3 \times 10^5$ | 30 | 0.94 | N |
| | 7 | −0.240 | 23 | $7.0 \times 10^5$ | 29 | 0.94 | N |
| | 20 | −0.080 | 23 | $5.0 \times 10^6$ | 24 | 0.94 | N |

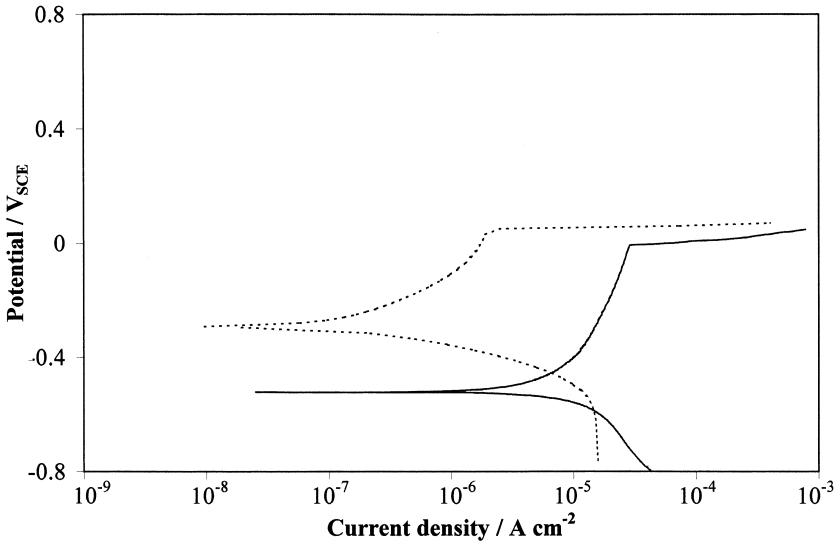


*Fig. 4.* Polarization curves recorded in blank solution after 45 min (dotted lines) or 20 days (solid lines) of immersion.

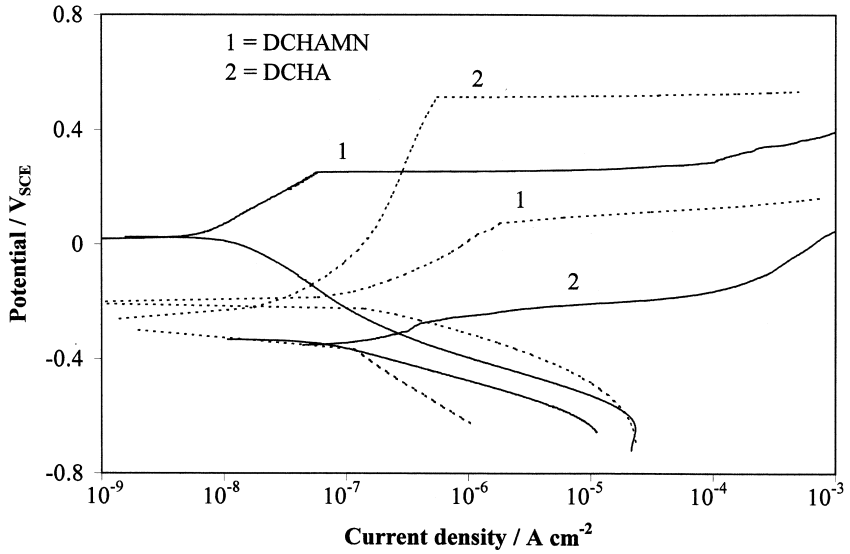


*Fig. 5.* Polarization curves recorded in DCHAMN (curves 1) or DCHA (curves 2) solutions after 45 min (dotted lines) or 20 days (solid lines) of immersion.

mation of a much more protective passive film, as the passive current densities were almost two magnitude orders lower than those recorded at short immersion times, and a much nobler corrosion potential was detected. The cathodic reaction was never inhibited.

DCHA showed quite a different behaviour: it was a very efficient anodic and cathodic corrosion inhibitor at short immersion times, but the protection was partially lost after 20 days of exposure, as a much more active breakdown potential ($E_b$) was exhibited and the cathodic reaction was no longer inhibited.

Table 3 collects the $E_{cor}$ and the $E_b$ values obtained under the various conditions and shows that localized corrosion attack developed not only in the blank solution, but also in the presence of DCHA or C6BTA, while DCHAMN, GPH or SN additions kept the steel electrodes under passive conditions throughout the immersion period, as substantiated by the relatively noble $E_{cor}$ and $E_b$ values.

*Table 3.* $E_{cor}$ and $E_b$ values measured from the polarization curves after different immersion times

| Environment | 45 min | | 20 days | |
|---|---|---|---|---|
| | $E_{cor}$ /V$_{SCE}$ | $E_b$ /V$_{SCE}$ | $E_{cor}$ /V$_{SCE}$ | $E_b$ /V$_{SCE.}$ |
| Blank = B | −0.294 | 0.056 | −0.520 | −0.007* |
| B + C6BTA | −0.340 | 0.332 | −0.415 | –* |
| B + DCHA | −0.262 | 0.512 | −0.344 | −0.264* |
| B + DCHAMN | −0.206 | 0.084 | 0.021 | 0.251 |
| B + GPH | −0.310 | 0.090 | −0.205 | 0.293 |
| B + SN | −0.308 | 0.410 | −0.135 | 0.379 |

* Localized attack is present before anodic polarization.

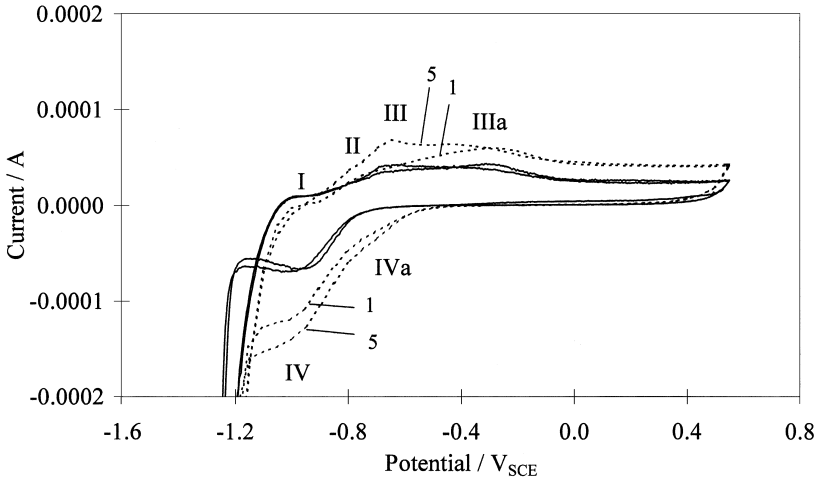


*Fig. 6.* CV in saturated calcium hydroxide solution (dotted lines) or in saturated calcium hydroxide solution containing 0.1 M chlorides and 0.05 M GPH (solid lines).

### 3.3. *Cyclic voltammetry*

The 1st and 5th cycle obtained in saturated calcium hydroxide in the absence of both additives and chlorides are shown in Figure 6 (dotted lines). Four anodic peaks were distinguishable, which can be interpreted on the basis of previous reports [6]. Peaks I and II were attributed to the oxidation of metallic iron to ferrous hydroxide; peaks III and IIIa were assigned to ferrous–ferric transformation in a hydrous outer oxide layer and in a relatively compact anydrous inner oxide layer, respectively. Two cathodic peaks were observed (IV and IVa), most likely conjugated to peaks III and IIIa, respectively. The cathodic peak connected to the reduction of ferrous hydroxide to iron became evident at high cycle numbers, while at low cycle numbers, like those shown in the Figure, it was obscured by water reduction.

In the presence of chlorides, a progressive deterioration of the electrode was seen, as more and more active breakdown potentials ($E_b$) were measured during each anodic sweep, with large hystereses for repassivation (Figure 7, dotted lines).

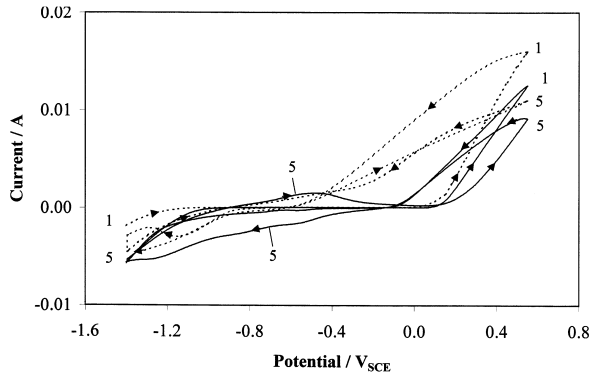


*Fig. 7.* CV in saturated calcium hydroxide solution containing 0.1 M chlorides (dotted lines) or in saturated calcium hydroxide solution containing 0.1 M chlorides and saturated DCHAMN (solid lines).

$E_b$ values over 0.55 V were obtained only in the presence of SN or GPH. As an example, the 1st and 5th cycles obtained in GPH solution are included in Figure 6 (solid lines). In the presence of DCHAMN, the $E_b$ and $E_r$ (repassivation potentials) values remained relatively noble and constant during each cycle, as may be seen in Figure 7 (solid lines). No inhibition of the localized attack was achieved in C6BTA or DCHA solutions, whose behaviour more or less overlapped that in the blank solution.

### 3.4. *FTIR spectroscopy*

The FTIR spectrum obtained by rubbing KBr powder on steel sheets, after three days of exposure to a saturated calcium hydroxide solution containing 0.05 M GPH, revealed the presence of glycerophosphate in the surface film. In fact, both the characteristic vibrations of $CH_2$ and CH groups at 2950–2850 $cm^{-1}$ and a broad band centred at 3400 $cm^{-1}$, connected to OH stretching, were clearly visible [7] (Figure 8(a), curve 1).

The spectrum obtained by diffuse reflectance on GPH powder (curve 2) showed remarkable differences in the region 1120–970 $cm^{-1}$, where some characteristic frequencies of the phosphate group fall [7] (Figure 8(b)). The GPH powder exhibited a strong band at 970 $cm^{-1}$, which corresponds to PO symmetric stretching, and two strong bands at 1120 and 1080 $cm^{-1}$, connected to the asymmetric stretch (two components). In the case of chemisorbed GPH, the component at 970 $cm^{-1}$ was still visible, while the asymmetric stretch vibration produced three components at 1110, 1090 and 1030 $cm^{-1}$.

According to the literature [8], the vibration mode connected to the PO asymmetric stretch is constituted by only one component in the case of $PO_4^{3-}$ ion, which has a tetrahedral symmetry, while two components occur in the case of substitution at one oxygen atom, which lowers the ion symmetry. This is the case of GPH, where the group $-CH_2-CH(OH)-CH_2OH$ is bound to one oxygen atom. An even lower symmetry was present in

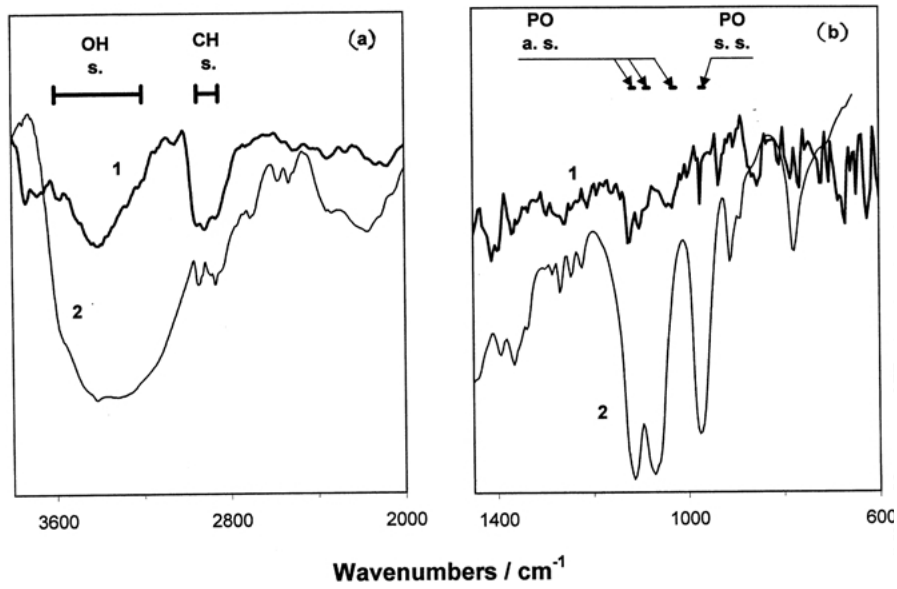


*Fig. 8.* FTIR diffuse reflectance spectra obtained after exposure of a steel sheet to a 0.05 M GPH solution (rubbing method, curve 1), or on GPH powder (curve 2). Ordinate represents transmittance.

chemisorbed GPH, as three components were present. This supports the hypothesis of a GPH anion which bridges two surface cations, to produce a surface polymeric complex (Figure 9(a)). In this case two equivalent groups and two different groups were bound to the central P atom.

Analysis of the FTIR spectra also showed that no GPH chemisorption was evident if GPH was dissolved in 0.1 M NaOH. This suggests that in saturated calcium hydroxide solution GPH is chemisorbed on steel mainly as a surface calcium complex. The presence of calcium ions trapped in the surface layer of the ferric oxide passive film formed in saturated calcium hydroxide solution has already been detected by other researchers [9, 10].

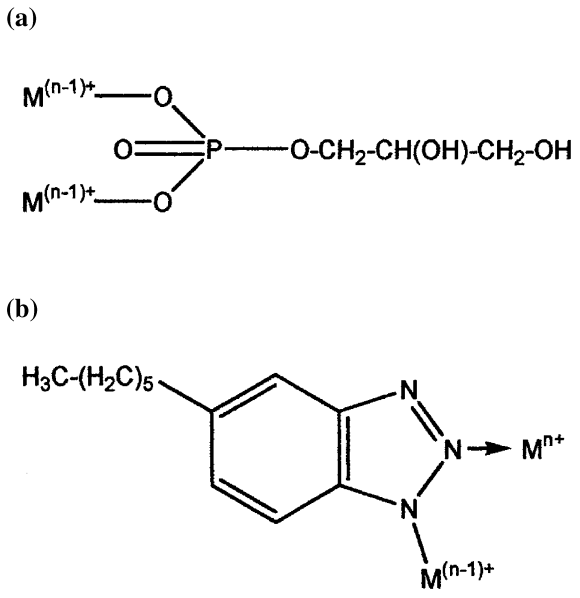


*Fig. 9.* Structures of the surface chelating complexes formed by chemisorbed GPH (a) or C6BTA (b).

Figure 10, curve 1 shows the spectrum obtained with the rubbing method after exposure of a steel sheet to a 0.005 M C6BTA solution, saturated by $Ca(OH)_2$. The presence of C6BTA was revealed by the peaks centred around 2920 $cm^{-1}$, associated with aliphatic CH stretching vibrations. Over these strong peaks, a large band between 3600 and 2400 $cm^{-1}$ was superimposed, which is attributed to the stretching of triazolic NH groups involved in intermolecular hydrogen bonds [11, 12]. Curve 2 is the reference spectrum obtained from C6BTA powder, where the presence of NH groups was much more evident and partially covered the vibrational bands associated with CH stretching. Similarly to the case of C6BTA chemisorbed on copper [12], these results suggest that C6BTA is chemisorbed on steel, through NH groups which dissociate and chelate surface cations. In Figure 10(b), another region of the same spectra is shown. Both spectra exhibited a peak at 1205 $cm^{-1}$ connected to N=N bond of the triazolic ring. However, spectrum 1 also exhibited a small new peak at 1170 $cm^{-1}$ which, like the case of copper (where this last peak becomes predominant) [11, 12], may be attributed to the same bond weakened by the formation of a coordinative bond with a surface cation.

Thus, C6BTA should inhibit steel corrosion in chloride-containing saturated calcium hydroxide solution by forming either a mono- or a bidentate surface complex (Figure 9(b)). The amount of surface complex formed on steel exposed to a NaOH solution of C6BTA was scarce. This suggests that surface complexation of calcium cation must also play a significant role in C6BTA chemisorption.

In Figure 11(a), the FTIR spectra obtained from liquid DCHA (curve 2) and from the surface products formed on steel in DCHA alkaline solution (curve 1) are compared. Both exhibited the NH stretching vibration, at frequencies over 3200 $cm^{-1}$, and the $CH_2$ stretching

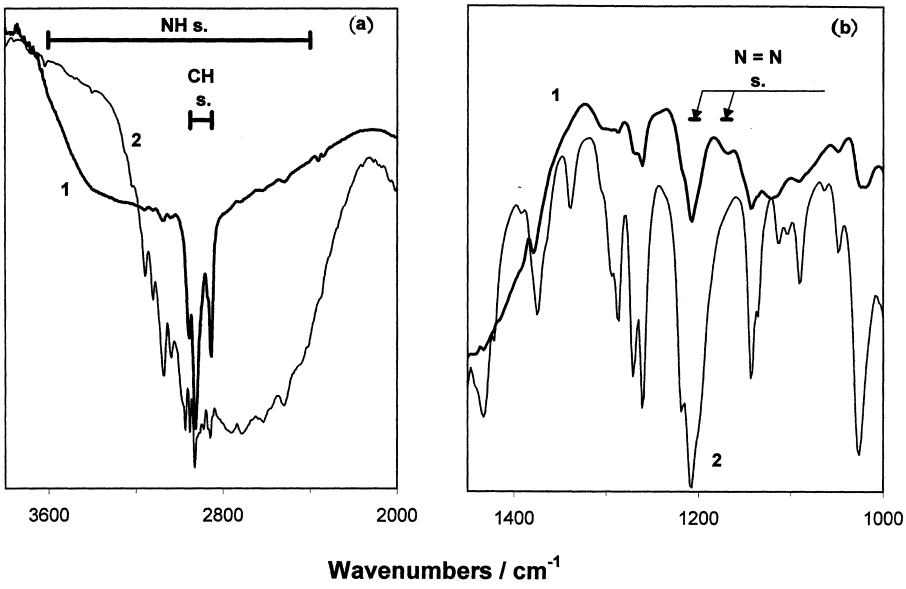


*Fig. 10.* FTIR diffuse reflectance spectra obtained after exposure of a steel sheet to a 0.005 M C6BTA solution (rubbing method, curve 1), or on C6BTA powder (curve 2). Ordinate represents transmittance.

bands in the range of 2850–2930 $cm^{-1}$ [7]. This supports molecule chemisorption on the steel surface, most likely through the electron lone pair on the nitrogen atom.

Figure 11(b) allows the same comparison in the case of DCHAMN: curve 1 is the spectrum obtained from the surface products formed during seven-day exposures to DCHAMN solution, while curve 2 was obtained from DCHAMN powder. Curve 1 is quite close to curve 1 of Figure 11(a): this suggests the presence of chemisorbed DCHA on steel exposed to DCHAMN solutions, most likely as a result of ammonium group hydrolysis [13]. Curve 2 confirms this hypothesis as it shows $NH_2^+$ stretching vibrations between 2700 and 3000 $cm^{-1}$, accompanied by multiple combination bands from 2700 down to 2300 $cm^{-1}$ [7], which are absent in curve 1. No clear indication of chemisorption appeared after only a three-day immersion in DCHAMN solution, indicating that the hydrolysis was a slow process.

## 4. Discussion

In saturated calcium hydroxide solution, where stable passive conditions are achieved, EIS spectra recorded on steel after a 20 day immersion are fitted by a simple RC parallel network, whose parameters are reported in Table 2 [14]. In the presence of chlorides, to this equivalent circuit a third parallel arm with a resistance

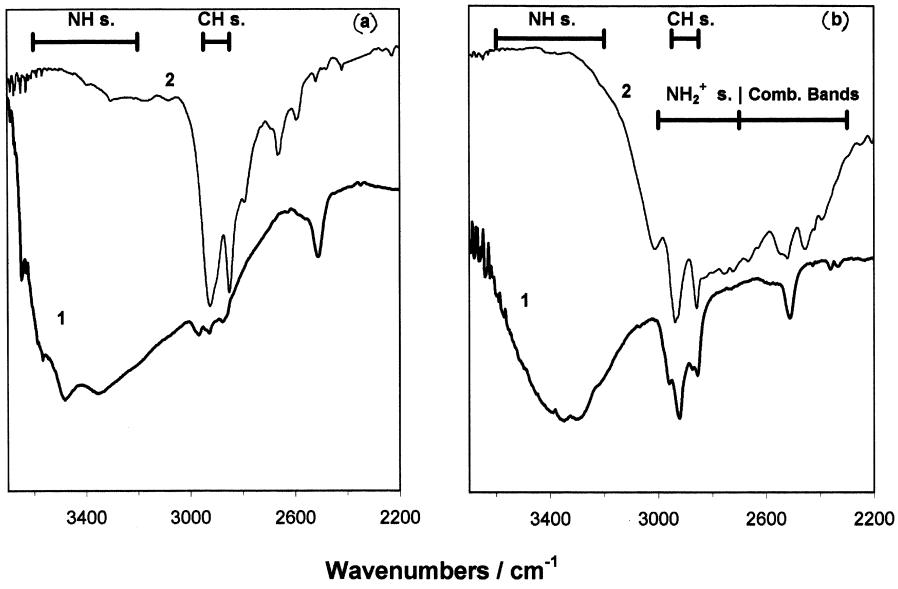


*Fig. 11.* (a) FTIR diffuse reflectance spectra obtained after exposure of a steel sheet to a saturated DCHA solution (rubbing method, curve 1), or on liquid DCHA (curve 2). (b) FTIR diffuse reflectance spectra obtained after exposure of a steel sheet to a saturated DCHAMN solution (rubbing method, curve 1), or on DCHAMN powder (curve 2). Ordinate represents transmittance.

and a Warburg element is added, whose presence is likely to be connected to the onset of diffusion limited processes caused by the build-up of corrosion products, at localized spots on the steel electrode. This suggests that in choride solution, the corrosion process is under mixed activation/mass transfer control. The $R_p$ values, reported in Tables 1 and 2, corresponding to the steel electrode polarization resistance, undergo a slight increase during the 20 day immersion, suggesting a reduction in corrosion rate with time. This could be a consequence of the build up of corrosion products over the pits, which may be partially obstructed. These corrosion products also induce an increase in the electrode surface area which causes the observed increase in the double layer capacitance values ($C_p$) of the steel electrode. The corrosion potentials become more and more active in time.

With GPH, DCHAMN or SN, which prevent localized corrosion, nobler corrosion potentials are found, and only one time constant is present throughout the immersion, indicating that the corrosion process is under activation control. This behaviour is similar to that observed on steel electrodes in calcium hydroxide solution in the absence of chlorides [14]. In the present study the equivalent circuit used to fit the experimental spectra is similar to that adopted in previous work [14], with a CPE instead of a pure capacitance, owing to time constant dispersion.

On the basis of FTIR findings, GPH protects the surface passive film by chelating surface cations, mainly calcium cations, through the phosphate group. In the field of industrial water treatment, synergetic inhibition between calcium cations and phosphate or phosphonate derivatives has been demonstrated [15]. CV tests suggest that this film is quickly formed, while EIS data show that its protectivity improves with time, because $R_p$ increases.

Nitrite is known to oxidize the ferrous ions to ferric oxide quickly, thus reinforcing the surface oxide film [16]. This mechanism accounts for the excellent corrosion inhibiting properties afforded by SN, as shown by all the electrochemical tests.

In DCHAMN, at short immersion times, the cationic part of the salt appears to have an adverse effect on the inhibiting properties of nitrite, that is the anionic part. In fact, CV tests show that, during the anodic polarization, much more efficient suppression of localized corrosion is achieved in SN solution than in DCHAMN solution, although both solutions contain more or less the same amount of nitrite anion. Moreover, EIS spectra recorded after one day of immersion in DCHAMN solution exhibit $R_p$ values which are one order of magnitude lower than those recorded in SN solution.

An opposite trend is found after seven and 20 day immersions, when $R_p$ values over $10^7\ \Omega\ cm^2$ are recorded in DCHAMN solution. On the basis of FTIR findings, immersions of over three days in DCHAMN solutions are required to allow hydrolysis of the salt and, as a consequence, DCHA chemisorption. It is possible that the excellent inhibiting efficiency achieved at that time is caused by a synergetic inhibition between chemisorbed DCHA and dissolved nitrite.

In DCHA or C6BTA solutions, steel corrosion potentials tend to decrease with time and pits are observed at long immersion times. The presence of two time constants in the EIS spectra at short immersion times suggests that the onset of pits is not delayed by these substances, which can only slow down the rate of localized corrosion. In both substances, chemisorption centres are nitrogen atoms belonging to an amino group, in the case of DCHA, or to a triazolic ring, in the case of C6BTA. It appears that these chemisorption centres produce less efficient inhibition than the phosphate group, present in GPH, although the contribution of other molecule parts cannot be excluded.

## 5. Conclusions

The techniques adopted to investigate the corrosion inhibition mechanism of DCHAMN, GPH, C6BTA and DCHA in saturated calcium hydroxide solution containing 0.1 M chlorides show that all of these substances are corrosion inhibitors which act by chemisorption. Only DCHAMN and GPH can completely prevent localized corrosion over 20 days of immersion. At short immersion times in DCHAMN solution, inhibition is mainly due to the anionic part of the salt, that is nitrite anion, which has oxidizing properties able to reinforce the surface oxide film. At long immersion times, excellent inhibiting properties are exhibited, due to a synergetic inhibition developed between nitrite and chemisorbed DCHA. The latter molecule is produced by slow hydrolysis of the salt.

The interaction between DCHA and the surface film most likely occurs through the electron lone pair of the nitrogen atom. GPH chemisorption occurs by the chelating action of the phosphate group with the surface cations, while C6BTA forms either mono- or, more rarely, bidentate surface complexes between triazolic nitrogen atoms and surface cations.

EIS tests show that inhibitors which can prevent pitting corrosion have similar spectra to those recorded in the absence of chlorides, and are characterized by a single time constant. On the contrary, substances able to delay, but not prevent, pitting corrosion have spectra with two time constants, like those obtained in the uninhibited chloride-containing solution.

## Acknowledgement

This research was co-financed by MURST funds.

## References

1. B. Elsener, 'Corrosion Inhibitors for Steel in Concrete, State of the Art Report', The European Federation of Corrosion (Maney Publishing, London, 2001).

2. C. Monticelli, A. Frignani and G. Trabanelli, *Cem. Concr. Res.* **30** (2000) 635.
3. Electrochemical impedance software Zplot for Windows® (1998).
4. A. Bonnel, F. Dabosi, C. Deslouis, M. Duprat, M. Keddam and B. Tribollet, *J. Electrochem. Soc.* **130** (1983) 753.
5. A. Frignani, G. Trabanelli, C. Wrubl and A. Mollica, *Corrosion* **52** (1996) 177.
6. J.T. Hinatsu, W.F. Graydon and F.R. Foulkes, *J. Appl. Electrochem.* **19** (1989) 868.
7. D. Lin-Vien, N.B. Colthup, W.G. Fateley and J.G. Grasselli, 'The Handbook of Infrared and Raman Characteristic Frequencies of Organic Molecules', (Academic Press, San Diego, CA, 1991).
8. G.M. Anthony, Proc. Corrosion 90, paper 97, NACE, Houston, TX (1990).
9. J.R. Gancedo, C. Alonso, C. Andrade and M. Gracia, *Corrosion* **45** (1989) 976.
10. C.J. Kitowski and H.G. Wheat, *Corrosion* **53** (1997) 216.
11. G.W. Poling, *Corros. Sci.* **10** (1970) 359.
12. G. Trabanelli, G. Brunoro, A. Frignani, F. Zucchi, C. Monticelli, G. Perboni, G. Rocchini, *Editions de la Révue de Métallurgie* **6** (1992) 219.
13. A. Phanasgaonkar, M. Forsyth and B. Cherry, Proc. 13th International Corrosion Congress, paper 178, Melbourne, Australia (1996).
14. C. Monticelli, A. Frignani, G. Brunoro, G. Trabanelli, F. Zucchi and M. Tassinari, *Corros. Sci.* **35** (1993) 1483.
15. E. Kàlmàn, I. Felhösi, F.H. Kàrmàn, I. Lukovits, J. Telegdi and G. Pàlinkàs, *in* M. Schütze (Ed.), Environmentally friendly corrosion inhibitors in 'Corrosion and Environmental Degradation' Vol. 1 (Wiley–VCH, Weinheim, 2000), p. 471.
16. A.M. Rosenberg and J.M. Gaidis, *Mater. Perform.* **18** (1979) 45.